The Effects of Corn Kernel Bio-Filler on the Fire Retardancy of Intumescent Fire-Retardant Coating for Steel Structures

Syed Niaz Hossain Chowdhury
Department of Mechanical Engineering, Universiti Teknologi PETRONAS, 32610, Bandar Seri Iskandar, Perak, Malaysia
syed_22012289@utp.edu.my

Faiz Ahmad
Department of Mechanical Engineering, Universiti Teknologi PETRONAS, 32610, Bandar Seri Iskandar, Perak, Malaysia
faizahmad@utp.edu.my (corresponding author)

K. E. Kee
Department of Mechanical Engineering, Universiti Teknologi PETRONAS, 32610, Bandar Seri Iskandar, Perak, Malaysia
keekokeng@utp.edu.my

Siti Haslina Ramli
GTS Petronas, Kuala Lumpur, Malaysia
sitihaslina@petronas.com

Received: 28 April 2025 | Revised: 9 June 2025 and 23 June 2025 | Accepted: 28 June 2025

 DOI: https://doi.org/10.48084/etasr.11794

ABSTRACT

The development of bio-based intumescent coatings is a focal point for achieving sustainability and eco-friendly coatings. This study introduces Corn Kernel (CK) bio-filler into a modified epoxy-based fire-retardant system, resulting in significant improvements in thermal resistance. This study develops intumescent coatings, utilizing CKs, and assesses the samples through thermal performance testing, char expansion analysis, and char morphology examination. The incorporation of 8% CK (CKC-8) enhanced the thermal performance of the coating, with a backside temperature recorded at 190.28 °C during the ASTM E119 test. Furthermore, the char expansion of the coating increased by 22.14%. The Thermogravimetric Analysis (TGA) examined the thermal pyrolysis behavior, revealing a 3% increase in residual mass. The Fourier Transform Infrared Spectroscopy (FTIR) and X-ray Diffraction (XRD) analyses confirmed the effective degradation of the CK, leading to the formation of $CaCO_3$ in the char. The Field Emission Scanning Electron Microscope (FESEM) images demonstrated the presence of cross-linked char structures within the CK-filled char samples.

Keywords-bio-filler; corn kernel; intumescent coating; fire resistance

I. INTRODUCTION

Steel is an important material in modern construction due to its durability and strength-to-weight ratio. However, in the event of a fire, steel becomes ductile, loses its 50% strength, and collapses in less than 1 h, when exceeding its threshold temperature of 500 °C [1]. Passive fire protective systems, both reactive and non-reactive, are utilized to address the safety challenges in the construction industry. Intumescent coatings are a system that swells and creates a barrier when steel is subjected to fire [2]. Intumescent fire-retardant coatings comprise three functional ingredients: ammonium polyphosphate functioning as an acid source, expandable graphite as a carbon source, and melamine as a blowing agent, incorporated in a resin binder with fillers. The homogenous mixture of these functioning materials involves a series of chemical reactions that create a multicellular insulation that prevents the heat from penetrating [3]. The carbonaceous char produced from the carbon source, EG, is catalyzed by the acid source, APP, to capture the non-volatile gases from the

blowing agent, MEL, resulting in the expansion of the char layer. The BA functions as an efficient additive in the coating [4, 5]. The incorporation of the bisphenol (BPA)-188 binder system, modified by PDMS, enhances the coating's efficacy in harsh environments while diminishing the presence of less harmful phenolic chemicals [6]. Fillers are a key component widely used in coating systems, which can significantly enhance the retardancy [7]. They undergo chemical or physical reactions and the residue they leave after combustion considerably creates insulation in the substrate [8, 9]. Compared to conventional fillers, biological and bio-based fillers tend to be sustainable and degrade without polluting the environment [7]. The inclusion of eco-friendly bio-derived material, such as Rubberwood Biomass Ash (RWA), Chicken Eggshells (CES), Clamshell (CS), and Shellfish Shells (SS), has extensively enhanced the thermal protection properties of the fire coating. These findings have shown improvement in the fire insulation barrier and good thermal resistance [3, 7, 10]. The reason behind this exceptional fire resistance in the intumescent system is the presence of both organic and inorganic phases of fillers and their compatibility with the matrix [11]. In addition, materials derived from crops, like rice and corn, show excellent thermal insulation and stability [10].

Authors in [12] investigated the performance of an alternative fire-resistant system of Rice Husk Ash (RHA) activated with alkali as a substitute for traditional geopolymer panels. When the RHA-filled samples were exposed to a continuously rising temperature, the glass transition temperature reached 120 °C (TG). Fire tests revealed that RHA activated with alkali sustained an indifferent surface temperature of around 75 °C for 5 h, which is preferable to the aerated geopolymer panels. Higher insulation was obtained at higher temperatures (up to 1000 °C) by the RHA-filled panels compared to the aerated geopolymer panels, which expanded 1.5–2.5 times. Authors in [13] synthesized C-6 position oxidized corn starch as a carbon source, incorporating microencapsulated ammonium polyphosphate, and evaluated its flame-retardancy. The inclusion of 6.25% oxidized corn starch and ammonium polyphosphate improved the LOI index by up to 7, enabling the UL94 V-0 rating for all composites. TGA revealed that the carboxyl content of starch affected its thermal stability and increased its char residues while decreasing its thermal stability. The highest char residue was 23.4%. The outcome of incorporating corncob biochar into composite materials was investigated in [14]. The biochar-containing specimens showed exceptional heat stability. Lower thermal conductivity was observed in the composite after 10% biochar was added. According to TGA, adding corncob biochar improved the quick drop and altered steadily at high temperatures. The cone calorimetry test indicated a 34.5% lower peak heat release rate. Authors in [15] evaluated the performance of flame retarded composites incorporated with corn husk fibers. The flame retardant lowered flammable gas during combustion, forming an intumescent carbon layer that isolated the hot oxygen. LOI increased as the mass fraction and flame-retardant homogeneity increased. It was reported that the LOI was 35.2%.

CKs are derived from corn cob having a starchy endosperm with 86%-89% starch and lower thermal conductivity [16]. However, their application in intumescent coatings is yet to be discussed. To address this gap, the CK bio-fillers were employed to enhance the efficacy of intumescent coatings. In this research, CK bio-fillers were prepared and further analyzed by FTIR and XRD to be applied apply as a synergistic agent in the coating. The coating samples (CKC) were evaluated for their fire-retardant performance via a fire test and char expansion test, and characterized by TGA, XRD, FTIR, and FESEM.

II. MATERIALS AND METHODS

A. Coating Materials

Corn was acquired from a corn harvesting farm located in Bota, Perak, Malaysia. Expandable Graphite (EG), Boric Acid (BA), Ammonium Polyphosphate (APP), Melamine (MEL), and Polydimethylsiloxane (PDMS) were procured from Sigma Aldrich, Malaysia. The binder system, consisting of Bisphenol A (BPA) resin and polyamide amine H-2310, was supplied by McGrowth Chemical, Malaysia. TSA Industries (Ipoh), Malaysia, provided the steel substrate A36M.

B. Modification of Epoxy

The BPA-188 and PDMS were measured at 70 wt% and 30 wt%, respectively. The epoxy was stirred and heated to 60 °C on a hot plate with a shear mixer for 30 min at 40 rpm to decrease viscosity and achieve a colorless condition. Subsequently, PDMS was incorporated into the epoxy and blended for 15 min. To enhance the interfacial adhesion of the blend, 2g of triethoxysilane was introduced to the mixture and stirred for 10 min. Subsequently, 6 drops of dibutyltin dilaurate were added in a lapse of 30 s to promote polymerization. The mixture was stirred for 30 min at 60 rpm until it exhibited a milky appearance [6].

C. Preparation of Coatings Samples

APP, MEL, and BA were accurately measured, as indicated in Table I, and subsequently mixed using a mixer for 40 s. EG was physically integrated into the mixture to ensure a homogeneous blend of the coating components and prevent mechanical damage. A stirring rod was used for 5 min to obtain a homogenous mixture. The CK, averaging 125 μm in particle size, was sieved by a laboratory sieve shaker and subsequently added to the mixture to achieve uniform dispersion. The proportion of the CK filler was adjusted to replace the binder percentage, maintaining the modified epoxy-to-hardener ratio of 2:1. The resulting mixture was then gradually incorporated into the siloxane-modified resin system and agitated for 30 min at 40 rpm. The hardener (PA-2310) was introduced into the mixture for 10 min at 45 rpm [6]. Upon achieving a homogeneous coating mixture, it was prepared for application onto the sandblasted steel substrate measuring 10 × 10 cm^2. The prepared coating was applied to the substrates with a brush, ensuring a uniform thickness across the substrate, leaving no uncoated corners. The coating was consistently maintained at an average thickness of 1.5-1.7 mm. The coated steels were placed for curing at room temperature for one day, with the environmental humidity recorded at approximately 89%.

TABLE I. MASS PERCENTAGES OF COATING INGREDIENTS

Sample	Coating ingredients						
	APP	EG	MEL	BA	CK	Resin	Hardener
CKC-0	11.23	5.5	5.5	11.11	--	44.44	22.22
CKC-2	11.23	5.5	5.5	11.11	2	43.11	21.55
CKC-4	11.23	5.5	5.5	11.11	4	41.77	20.89
CKC-6	11.23	5.5	5.5	11.11	6	40.44	20.22
CKC-8	11.23	5.5	5.5	11.11	8	39.11	19.55
CKC-10	11.23	5.5	5.5	11.11	10	37.77	18.89

D. Characterization of Coating Samples

1) Laboratory Scale Fire Performance Test (ASTM E-119)

The ASTM E119 test assessed the heat penetration in the steel substrates at elevated temperatures. A distance of 7 cm was maintained from a portable butane torch and exposed to ignition for 60 min. Three K-type thermocouples are affixed to the backside of the coated substrates with RTV Silicone (tolerance up to 650°F) adhesive, as seen in Figure 1 [18]. The high-temperature blue flame was sustained during the test to ensure that the flame temperature was above 1100 °C [17]. The changes in temperature in the substrate were recorded through a data logger connected to a computer at 1-min intervals.

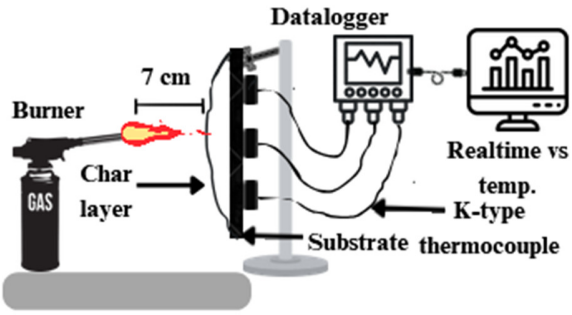

Fig. 1. Schematic diagram of ASTM E-119 fire test.

2) Coating Expansion Test

A Carbolite Gero muffle furnace, model CWF 13/13, featuring a temperature range of 30 °C-1300 °C, was used to examine the physical characteristics and expansion of the char. The sample thickness was measured before and after charring, and an Intumescent Factor (IF) was computed based on the reported thickness [3]. The formulation is as given in:

$$IF = \frac{d_2 - d_0}{d_1 - d_0} \quad (1)$$

where d_0 represents the substrate thickness, d_1 denotes the coating thickness of the substrate, and d_2 is the char expansion. The sample applied to the steel substrate (5×5 cm²) was heated to 600 °C at ambient temperature at a rate of 20 °C/min. The temperature was maintained for 60 min to allow the coating to swell properly and degrade all the ingredients. The sample was kept in the furnace for at least 6 h at 25 °C to avoid the thermal shock. The expansion of the coating was measured using slide calipers, and the char was inspected considering the adhesion to the steel substrate, color, and cracks that occurred on the char.

3) Thermogravimetric Analysis

The TGA evaluated the thermal degradation of the coatings by analyzing their residual mass. The coating sample was crushed, and approximately 10 mg was taken for the test. The analysis was conducted in a controlled nitrogen environment at a heating rate of 10 °C/min and a flow rate of 20 ml/min over a temperature range of 25-800 °C using a Q50 PerkinElmer thermal analyzer [19].

4) Characterization of Char Residue

a) X-Ray Diffraction Analysis

The XRD analysis was conducted to analyze the degraded compounds in the char residue in the char expansion test and the crystallinity of these compounds. As for the char, 2-3 mg of it was extracted and placed on the sample holder. This analysis was conducted utilizing Copper Kα radiation and a nickel filter within the $10<2\theta<90$ range.

b) Fourier Transform Infrared Spectroscopy

FTIR was employed to identify the functional groups of a molecule based on the IR absorption frequencies associated with those groups. FTIR spectra were obtained in the range of 400-4000 cm-1, and the observed peaks were evaluated. Approximately 2 grams of the char were utilized for analysis in the EQUINOX55 FTIR spectrometer employing KBr pellets.

5) Field Emission Scanning Electron Microscope

The FESEM model SUPRA 55VP was used to analyze the morphology of the degraded char. Throughout the test, the magnification ranged from 50X to 2000X.

III. RESULTS AND DISCUSSION

A. Fire Retardancy Performance of Coatings

The evaluation of the fire retardancy of the coated samples was performed through fire testing in accordance with the ASTM E-119 standard. It was found that the backside temperatures for all coating samples exhibited identical temperature patterns, as depicted in Figure 2. In the first 5 min of the test, the temperature increased rapidly on the substrate's backside. This indicates that the early breakdown of the coating materials resulted in a multi-porous char layer, even when the substrate temperature remained below 170 °C. The temperature escalated swiftly during the charring process, until the 15th min. After the 15th min, except for the sample CKC-6, all the CK-filled coatings showed a decreased substrate temperature. However, the temperature for CKC-6 started to decline after the 20th min. The temperature increases for the control formulation CKC-0 continued till the 40th min due to fragile and soft char. In the 15th min, the temperature of the CK-filled coating sample was recorded as being almost 30% lower than that of the control formulation. The highest backside temperature recorded for the control formulation was 308.86 °C after the 1-h fire test, 38% higher than that of the best formulation, CKC-8. The backside temperature of CKC-8 was recorded at 190.28 °C. Regarding the other coated samples, backside temperature was recorded at 265.3 °C, 227.14 °C, 205.58 °C, and 208.4 °C, for CKC-2, CKC-4, CKC-6, and CKC-10, respectively. Nevertheless, the inclusion of CK bio-filler has cross-linked with carbon atoms, creating a highly

dense char. However, a 10% inclusion of CK could be the threshold for adding it as a filler, which results in fragile char and leads to poor fire performance. The early degradation of the epoxy system created compactness in the char while constituents of CK pyrolyzed to non-combustible gases that could suppress the smoke and heat penetration to the substrate. A potential mechanism can be the synergistic effects of the coating ingredients (APP, MEL, BA) and CK. The degradation of APP and MEL released NH_3 and N_2 around 350 °C, and parallelly, BA decomposed to B_2O_3 around 300 °C [20]. The calcium oxalate (C2CaO4) decomposed to $CaCO_3$, which later degraded to CaO and released CO_2 at an elevated temperature [21]. This observation shows that samples filled with CKs were more fire-resistant, stopping the heat penetration.

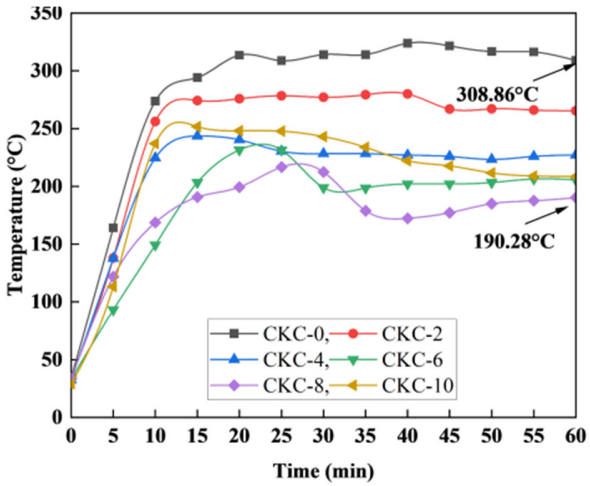

Fig. 2. Evaluation of the backside temperature versus time of coated samples.

B. Analysis of Char Appearance and Expansion

The IF and the char appearance are illustrated in Figures 3 (a) and (b), respectively. The coating samples turned brown after undergoing a furnace test. For the control formulation CKC-0, the IF value was 4.49, whereas for CKC-8, the IF value was 5.51, which is 22.72% higher. The highest IF value of 6.12 was calculated for CKC-6. The IF values for the other samples were 5.2, 5, and 5.44 for CKC-2, CKC-4, and CKC-10, respectively. CKC-0, possessing a lower IF value, exhibited significant cracks and voids in the char, resulting in heat penetration. CKC-6 exhibited a larger IF value, leading to a comparatively greater enhancement in the char compactness than CKC-0. Nevertheless, CKC-8, possessing a moderate IF value, exhibited a more compact, uniform char structure with significantly smaller voids. This indicates that both lower and higher values of IF result in more cracks, making them less effective than the intermediate IF value [22]. For CKC-0, it was reported that the char was loose and detached from the substrates, whereas the CK-filled samples showed relatively compact char and good adhesion.

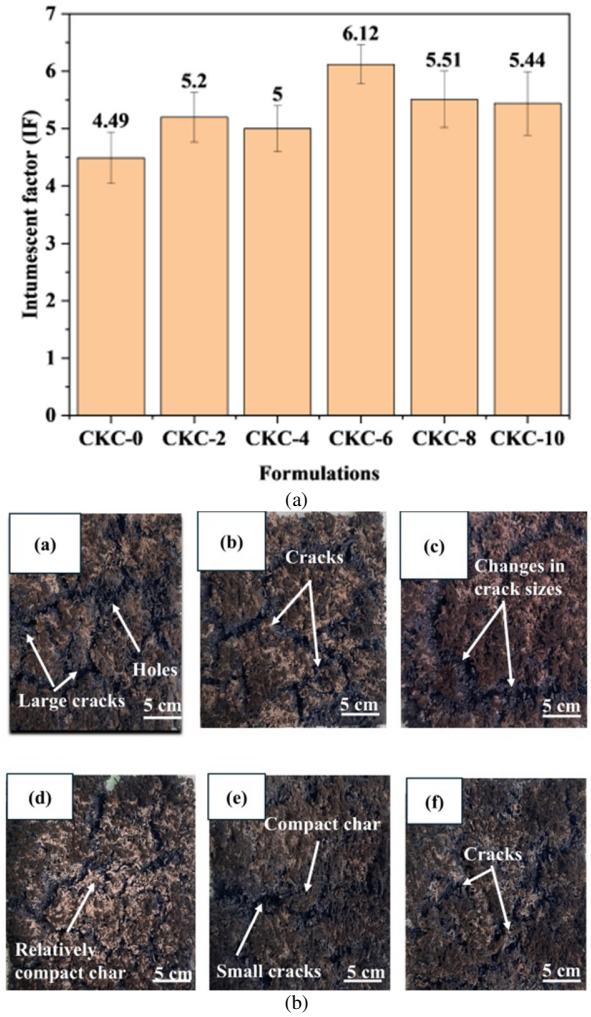

Fig. 3. (a) Intumescent factor and (b) physical characteristics of char.

C. Analysis of Char Residue Composition

The evaluation of the char composition of degraded ingredients was performed by XRD analysis. Figure 4 (a) depicts the diffraction pattern for the samples CKC-0, CKC-4, CKC-6, and CKC-8. The peaks were found to be almost symmetrical in the spectrum. Graphite (C, ICDD reference no. 98-008-8813) was identified in the orthorhombic form at 2θ = 14.80° (d spacing = 5.97 Å). The peaks recorded at 2θ = 24.40° (d spacing 3.64), validated the existence of tetragonal boron phosphate (BPO_4) in the char residue [23]. Hexagonal boron nitride (h-BN, ICDD reference no. 98-018-6246) was ascribed at peak 2θ = 26.69° with the d spacing value of 3.33 Å [24]. Inorganic sassolite (H_3BO_3, ICCD reference no. 98-002-4711) was recorded at a peak 2θ=28.02° (d spacing 3.18 Å) in its anorthic form [23]. Carbonate mineral "Calcite" ($CaCO_3$, ICCD reference no.00-005-0586) was ascribed at peak 2θ = 39.40° (d spacing 2.28 Å) [25]. Crystallinity was increased after the inclusion of the CK. Crystallinity was 70% for CKC-0, whereas for CKC-8, crystallinity increased to 78.09%. It was observed that the IF value increased with crystallinity, while the backside temperature decreased as crystallinity increased. This defines the successive effects of the CK as a bio-filler.

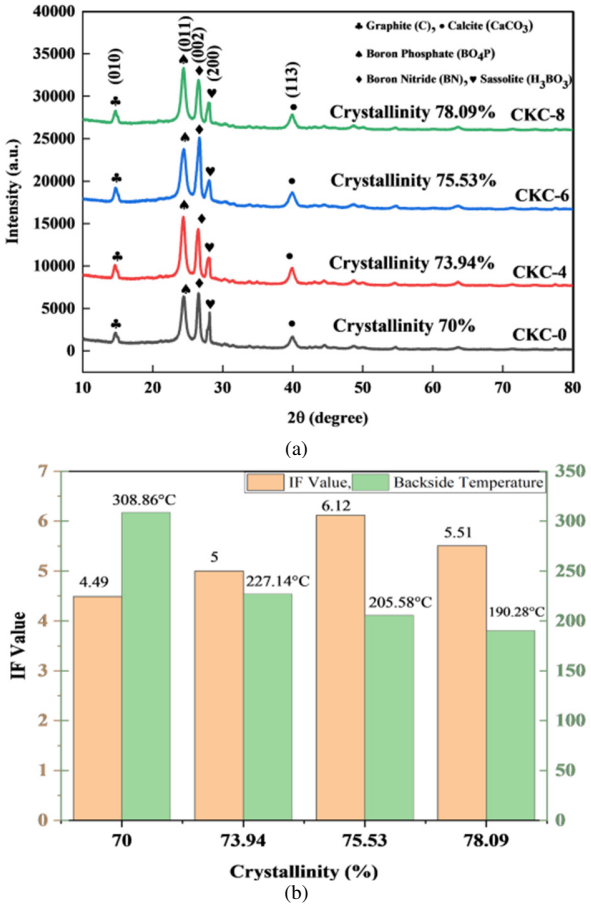

Fig. 4. (a). XRD spectrum of char residue, and (b) co-relation of crystallinity with IF value and backside temperature.

Figure 5 illustrates the FTIR patterns of the char samples for CKC-0, CKC-2, CKC-4, CKC-6, CKC-8, and CKC-10. The inclusion of CKs has improved the coating performance by slightly varying the functional groups in the char residue. The spectra for the reference sample CKC-0 show ten vibration bands, while eleven bands are present in the CK-filled coating samples. Strong vibration bands at 3429 cm-1 and 3208 cm-1 define the (O-H) group in the char that remained stable after a fire test [26]. Phosphate (PO_4) was observed at 1184 cm-1 in the (P-O-P) region between 1400-900 cm-1 [27]. In the (P-O-P) chain, vibration bending was observed at 920 cm-1 for (P-O) vibration, whereas at 1091 cm−1, the symmetric vibration was present [26]. The presence of these phosphatic groups resulted from the degradation of APP and the polyamide hardener [22]. The δ(B-O-P) band in the borate region was observed at 626 cm−1 [23]. The absorption band at 547 cm-1 was ascribed to the δ(O-B-O) region [23]. The vibration band at 2264 cm-1 was assigned to the (C=N) group [10]. It can be justified that the degradation of polyamide hardener in the coating has resulted in this nitrile group. Stretching peaks at 1644 and 1429 cm-1 were assigned to the (C=C) and (C=O) bond, respectively, due to the amorphous carbon present in the amine and graphite in the coating [18].

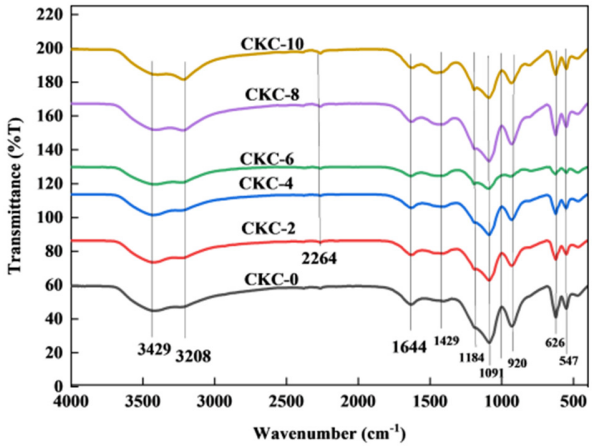

Fig. 5. FTIR spectra of CK-filled intumescent fire-retardant coating.

D. Analysis of Coating Thermal Stability

The coated samples were subjected to thermogravimetric measurement in order to evaluate their thermal stability. Figure 6 (a) illustrates the changes in residual mass versus temperature at 800°C. The recorded final residue mass for the formulations CKC-0, CKC-2, CKC-4, CKC-6, CKC-8, and CKC-10 has been found to be 35.7%, 38.4%, 37.5%, 38.3%, 38.5%, and 36.6%, respectively. In comparison to the reference formulation, the thermal stability of CKC-8 was enhanced by 7.84% due to the inclusion of the filler.

However, the influence of the CK is not significant due to its earlier degradation at high temperatures. The coating degraded in four stages: melting, intumescence, char formation, and degradation [3]. The TGA graph showed a mass loss of almost 2-5% between 0 °C and 140 °C. BA starts to degrade at 134 °C [18]. A significant mass loss, or roughly 25-33%, was observed between 140 °C and 390 °C. This stage involves decomposing the coating ingredients, such as APP, MEL, and epoxy, and eliminating the water content or chemical absorption. The significant mass loss for the control formulation CKC-0 started at 135 °C, whereas for CKC-8, it was 140 °C. This confirms the thermal improvement achieved by the inclusion of the CK filler. The DTG curves for the coating samples CKC-0, CKC-2, CKC-4, CKC-6, CKC-8, and CKC-10 are presented in Figure 6 (b). For all coating samples, 4 degradation stages were noticed. In the first stage, degradation occurred from 100 °C to 150 °C, attributed to the degradation of the polyamide hardener at 124 °C, the thermal decomposition of BA, and the elimination of water [20]. BA tends to start dehydrating at 129 °C. The decomposition in the second stage can be observed in temperatures between 220 °C and 350 °C. This resulted from the degradation of MEL at 290 °C and ammonium APP at 350 °C that releases N_2 and NH_3 in the event [22]. The third stage of decomposition was found from 350 °C to 400 °C due to the degradation of the polymeric system and the breakdown of EG contents at 371 °C in the coatings [22]. In the final stage, the phosphorus derivatives decomposed above 500 °C [23].

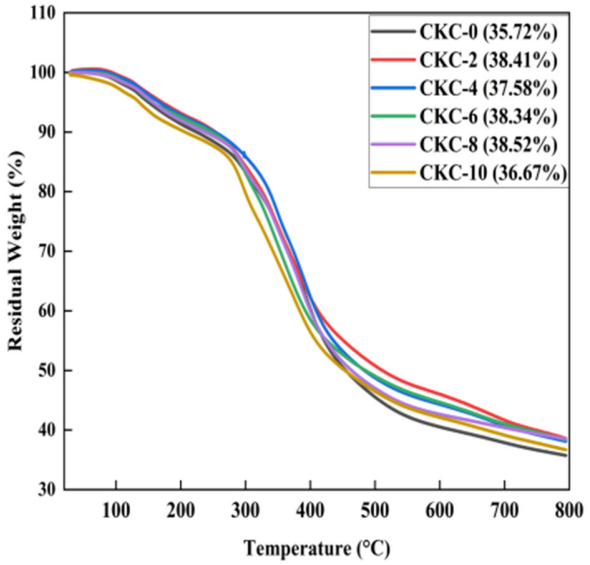

(a)

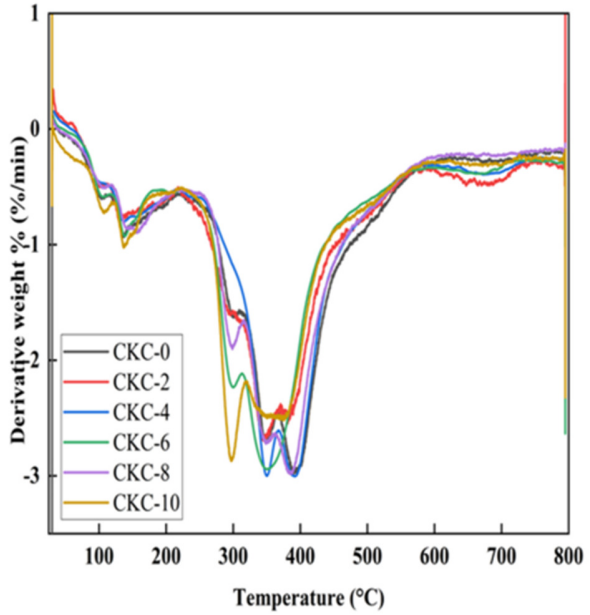

(b)

Fig. 6. (a) TGA of coating samples, and (b) DTG of coating samples.

E. Morphology Analysis of Char Residue

FESEM was performed to examine the char morphology following the fire test in Figure 7 (a) and (b), which has numerous fractures and large pores on the surface of the sample CKC-0. The irregular char structure and the existence of voids and loose structures contribute to poor fire performance [24]. The char adhesion is decreased by irregular char formations, which also make it more difficult to trap gases and penetrate heat [23]. A more distinct and compact char structure was obtained for the sample CKC-8 in Figure 7 (c) and (d). The reduction in the crack size and honeycomb-like char structure led to a better thermal performance of the coating [23]. Gaseous compounds like- CO_2, NH_3, and N_2 were emitted due to the thermal decomposition of APP, MEL, and BA, and the dehydration of epoxy resin in the coating that was trapped during char formation [22]. Sample CKC-8 exhibited a significant quantity of bubbles, indicating that the inclusion of CK has enhanced the gas entrapment ability and spongy texture in the char, strengthening the bonding with the substrate and increasing the heat shielding [6]. Nevertheless, the presence of microscale cracks and pores entrap the gases and disrupt the continuous heat transfer. The formation of the silicate network makes the char structure more compact and stable [18].

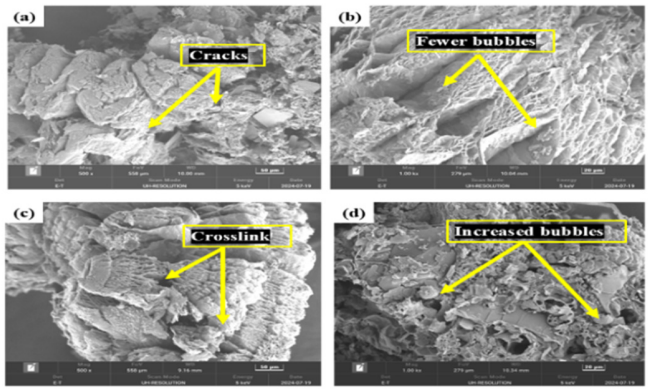

Fig. 7. FESEM of char structure of CKC-0 (a) and (b), and compact char of CKC-8 (c) and (d).

IV. CONCLUSION

In this research, a bio-based coating system was developed using Corn Kernels (CKs) to replace conventional inorganic fillers. The char quality was improved, and the lower backside temperature in ASTM E119 was recorded at 190.28 °C. Authors in [18] used zirconium phosphate as a filler and recorded a substrate backside temperature of 219 °C in the ASTM E119 test. This study utilized bio-filler CKs, which showed a 13.11% lower backside temperature compared to the results reported in [18]. The furnace test identified a dense char and increased IF values in the CK-filled coating samples. Notably, the Thermogravimetric Analysis (TGA) affirmed a higher residual mass for CKC-8, which was 38%. The combined analysis of the Fourier Transform Infrared Spectroscopy (FTIR) and X-ray Diffraction (XRD) findings indicates the presence of high-temperature compounds, such as boron phosphate, boron nitride, and calcium carbonate, in the coating char, which slowed the heat penetration to the substrate. The Field Emission Scanning Electron Microscope (FESEM) revealed a denser and more compact char structure having a silica network within the CK-filled coating. Accumulating the findings, this study demonstrates that the bio-filler CK has a significant influence on the formulation of sustainable and durable coating with improved efficiency. This study contributes to extensive research on environment-friendly bio-derived materials for coatings, as opposed to the expensive synthetic fillers. Future studies may focus on optimizing the filler material and particle size.

ACKNOWLEDGMENT

The authors acknowledge Yayasan UTP for the financial support provided under grant no. 015LC0-336.

REFERENCES

[1] M. M. Kharnoob, A. Al Zand, D. H. Khalaf, and L. M. Sabti, "Performance of Steel Beams reinforced by CFRP Sheets with Fire-Retardant Coating," *Engineering, Technology & Applied Science Research*, vol. 14, no. 6, pp. 18902–18910, Dec. 2024, https://doi.org/10.48084/etasr.8807.

[2] Z. Zhou, Z. Zhang, J. Huang, and Y. Wang, "Water-based intumescent fire resistance coating containing organic-modified glass fiber for steel structure," *Journal of Cleaner Production*, vol. 442, Feb. 2024, Art. no. 140897, https://doi.org/10.1016/j.jclepro.2024.140897.

[3] Y. Li, Y. Feng, Z. Xu, L. Yan, X. Xie, and Z. Wang, "Synergistic effect of clam shell bio-filler on the fire-resistance and char formation of intumescent fire-retardant coatings," *Journal of Materials Research and Technology*, vol. 9, no. 6, pp. 14718–14728, Nov. 2020, https://doi.org/10.1016/j.jmrt.2020.10.055.

[4] T. Wibawa *et al.*, "Enhancing the Mechanical and Fire-Resistant Properties of GFRP Composite using Boric Acid and Sodium Silicate Fillers," *Engineering, Technology & Applied Science Research*, vol. 14, no. 6, pp. 18911–18922, Dec. 2024, https://doi.org/10.48084/etasr.9271.

[5] A. Rakhman, K. Diharjo, W. W. Raharjo, V. Suryanti, and S. Kaleg, "Improvement of Fire Resistance and Mechanical Properties of Glass Fiber Reinforced Plastic (GFRP) Composite Prepared from Combination of Active Nano Filler of Modified Pumice and Commercial Active Fillers," *Polymers*, vol. 15, no. 1, Dec. 2022, Art. no. 51, https://doi.org/10.3390/polym15010051.

[6] Y. X. Lee, F. Ahmad, S. Karuppanan, C. Sumby, C. A. Shahed, and S. H. Ramli, "Thermo-mechanical performance of wolframite mineral reinforced siloxane-modified epoxy-based intumescent coating for structural steel," *Polymers for Advanced Technologies*, vol. 35, no. 1, Jan. 2024, Art. no. e6279, https://doi.org/10.1002/pat.6279.

[7] W. Zhan *et al.*, "Biomaterials in intumescent fire-retardant coatings: A review," *Progress in Organic Coatings*, vol. 192, Jul. 2024, Art. no. 108483, https://doi.org/10.1016/j.porgcoat.2024.108483.

[8] K. Diharjo, F. Gapsari, A. Andoko, M. N. Wijaya, S. Mavinkere Rangappa, and S. Siengchin, "Flammability and thermal resistance of Ceiba petandra fiber-reinforced composite with snail powder filler," *Polymer Composites*, vol. 45, no. 6, pp. 4947–4960, Apr. 2024, https://doi.org/10.1002/pc.28100.

[9] K. Diharjo, Sutrisno, Triyono, R. Afandi, and D. A. Himawanto, "Enhancing of fire resistance on CFRP using Sokka-clay particle for lightweight car body panel," in *2014 International Conference on Electrical Engineering and Computer Science (ICEECS)*, Kuta, Bali, Indonesia, Nov. 2014, pp. 188–192, https://doi.org/10.1109/ICEECS.2014.7045243.

[10] J. H. Beh, M. K. Yew, M. C. Yew, and L. H. Saw, "Characterization and fire protection properties of rubberwood biomass ash formulated intumescent coatings for steel," *Journal of Materials Research and Technology*, vol. 14, pp. 2096–2106, Sep. 2021, https://doi.org/10.1016/j.jmrt.2021.07.103.

[11] M. C. Yew, M. K. Yew, L. H. Saw, T. C. Ng, R. Durairaj, and J. H. Beh, "Influences of nano bio-filler on the fire-resistive and mechanical properties of water-based intumescent coatings," *Progress in Organic Coatings*, vol. 124, pp. 33–40, Nov. 2018, https://doi.org/10.1016/j.porgcoat.2018.07.022.

[12] K. Dhasindrakrishna, S. Ramakrishnan, K. Pasupathy, and J. Sanjayan, "Synthesis and performance of intumescent alkali-activated rice husk ash for fire-resistant applications," *Journal of Building Engineering*, vol. 51, Jul. 2022, Art. no. 104281, https://doi.org/10.1016/j.jobe.2022.104281.

[13] S. Zhang, F. Liu, H. Peng, X. Peng, S. Jiang, and J. Wang, "Preparation of Novel c-6 Position Carboxyl Corn Starch by a Green Method and Its Application in Flame Retardance of Epoxy Resin," *Industrial & Engineering Chemistry Research*, vol. 54, no. 48, pp. 11944–11952, Dec. 2015, https://doi.org/10.1021/acs.iecr.5b03266.

[14] J. Y. Choi, Y. U. Kim, J. Nam, S. Kim, and S. Kim, "Enhancing the thermal stability and fire retardancy of bio-based building materials through pre-biochar system," *Construction and Building Materials*, vol. 409, Dec. 2023, Art. no. 134099, https://doi.org/10.1016/j.conbuildmat.2023.134099.

[15] L. Lv et al., "Extraction of discarded corn husk fibers and its flame retarded composites," *Tekstil ve Konfeksiyon*, vol. 27, no. 4, pp. 408–413, Jul. 2017.

[16] S. García-Lara, C. Chuck-Hernandez, and S. O. Serna-Saldivar, "Development and Structure of the Corn Kernel," in *Corn (Third Edition)*, O. S. Sergio, Ed., Elsevier, 2019, pp. 147–163.

[17] J. Zhang *et al.*, "Preparation and performance analysis of palygorskite reinforced silicone-acrylic emulsion-based intumescent coating," *Progress in Organic Coatings*, vol. 166, May 2022, Art. no. 106801, https://doi.org/10.1016/j.porgcoat.2022.106801.

[18] Y. X. Lee, F. Ahmad, S. Kabir, P. J. Masset, E. Onate, and G. H. Yeoh, "Synergistic effects of tubular halloysite clay and zirconium phosphate on thermal behavior of intumescent coating for structural steel," *Journal of Materials Research and Technology*, vol. 18, pp. 4456–4469, May 2022, https://doi.org/10.1016/j.jmrt.2022.04.097.

[19] S. Kaleg *et al.*, "Evaluations of Aluminum Tri-Hydroxide and Pristine Montmorillonite in Glass Fiber Reinforced Polymer for Vehicle Components," *International Journal of Automotive and Mechanical Engineering*, vol. 19, no. 1, pp. 9379–9390, Mar. 2022, https://doi.org/10.15282/ijame.19.1.2022.02.0721.

[20] J. B. Zoleta *et al.*, "Improved pyrolysis behavior of ammonium polyphosphate-melamine-expandable (APP-MEL-EG) intumescent fire retardant coating system using ceria and dolomite as additives for I-beam steel application," *Heliyon*, vol. 6, no. 1, Jan. 2020, Art. no. e03119, https://doi.org/10.1016/j.heliyon.2019.e03119.

[21] T. Franke and T. Volkmer, "Mineralization treatment of European oak heartwood with calcium oxalate for improved fire retardancy," *Holzforschung*, vol. 76, no. 1, pp. 77–88, Jan. 2022, https://doi.org/10.1515/hf-2021-0055.

[22] S. Ullah *et al.*, "Effects of expandable graphite on char morphology and pyrolysis of epoxy based intumescent FIRE-RETARDANT coating," *Journal of Applied Polymer Science*, vol. 138, no. 41, Nov. 2021, Art. no. 51206, https://doi.org/10.1002/app.51206.

[23] Q. F. Gillani *et al.*, "Thermal degradation and pyrolysis analysis of zinc borate reinforced intumescent fire retardant coatings," *Progress in Organic Coatings*, vol. 123, pp. 82–98, Oct. 2018, https://doi.org/10.1016/j.porgcoat.2018.05.007.

[24] Z. Yang *et al.*, "Synergistic decoration of organic titanium and polydopamine on boron nitride to enhance fire resistance of intumescent waterborne epoxy coating," *Colloids and Surfaces A: Physicochemical and Engineering Aspects*, vol. 621, Jul. 2021, Art. no. 126561, https://doi.org/10.1016/j.colsurfa.2021.126561.

[25] F. Wang, H. Liu, and L. Yan, "Comparative Study of Fire Resistance and Char Formation of Intumescent Fire-Retardant Coatings Reinforced with Three Types of Shell Bio-Fillers," *Polymers*, vol. 13, no. 24, Dec. 2021, Art. no. 4333, https://doi.org/10.3390/polym13244333.

[26] D. Wu, M. Yang, T. Wu, Y. Shen, and T. Wang, "Green one-step modification of spent coffee grounds as synergistic bio-based flame retardant for waterborne epoxy resin," *Progress in Organic Coatings*, vol. 191, Jun. 2024, Art. no. 108409, https://doi.org/10.1016/j.porgcoat.2024.108409.

[27] Z. Xu, D. Liu, L. Yan, and X. Xie, "Synergistic effect of sepiolite and polyphosphate ester on the fire protection and smoke suppression properties of an amino transparent fire-retardant coating," *Progress in Organic Coatings*, vol. 141, Apr. 2020, Art. no. 105572, https://doi.org/10.1016/j.porgcoat.2020.105572.